Direct Measurement of Sheet Resistance $R_\square$ in Cuprate Systems: Evidence of a Fermionic Scenario in a Metal-Insulator Transition

P. Orgiani,[1] C. Aruta,[2] G. Balestrino,[2] D. Born,[3,5] L. Maritato,[4] P. G. Medaglia,[2] D. Stornaiuolo,[5] F. Tafuri,[3,5] and A. Tebano[2]

[1]*CNR-INFM Supermat and Department of Physics, University of Salerno, Baronissi (SA), Italy*
[2]*CNR-INFM Coherentia and Department of Mechanical Engineering, University of Roma Tor Vergata, Roma, Italy*
[3]*Department of Information Engineering, Second University of Napoli, Aversa (CE), Italy*
[4]*CNR-INFM Coherentia and Department of Physics, University of Salerno, Baronissi (SA), Italy*
[5]*CNR-INFM Coherentia and Department of Physics, University of Napoli, Napoli, Italy*

(Received 25 October 2006; published 16 January 2007)

The metal-insulator transition (MIT) has been studied in $Ba_{0.9}Nd_{0.1}CuO_{2+x}/CaCuO_2$ ultrathin cuprate structures. Such structures allow for the direct measurement of the 2D sheet resistance $R_\square$, eliminating ambiguity in the definition of the effective thickness of the conducting layer in high temperature superconductors. The MIT occurs at room temperature for experimental values of $R_\square$ close to the 25.8 kΩ universal quantum resistance. All data confirm the assumption that each $CaCuO_2$ layer forms a 2D superconducting sheet within the superconducting block, which can be described as weak-coupled equivalent sheets in parallel.

DOI: 10.1103/PhysRevLett.98.036401 PACS numbers: 71.30.+h, 74.78.Bz, 74.78.Fk

The basic features of the metal-insulator transition (MIT) in high temperature superconductors (HTSs) remain the subjects of ongoing discussion. In ultrathin films of low temperature superconductors (LTSs), the onset of superconductivity was found to occur when the normal-state sheet resistance $R_\square$ was smaller than the critical value of $h/4e^2 = 6.45$ kΩ [1–3]. A theoretical model based on quantum fluctuations of the order-parameter phase difference in a network of conducting clusters coupled by Josephson tunnelling junctions has been proposed [4,5] to explain MIT in ultrathin films. In this model the increase of the normal-state resistance is associated with an increase in quantum fluctuations of the superconducting phase. Eventually, these fluctuations destroy the global phase coherence and lead to an insulating state. It can be shown that a localization of the phase difference across the junction which occurs when the normal-state sheet resistance falls below a threshold value [6–9] $R_\square^{\mathrm{Tr}}$ of $h/4e^2$ gives rise to the superconductivity [10,11]. Recently it has been unambiguously verified that the MIT transition in these systems is driven by changes in intrinsic dissipation rather than being related to the film disorder [3]. An alternative explanation for the MIT is related to the renormalization of the interelectron interaction in the Cooper channel by the long-range Coulomb repulsion specific to dirty two-dimensional (2D) superconductors. In this case, it can be shown that the MIT occurs when the charge carrier density is so low that the mean free path of the electrons becomes smaller than the interatomic distance ($k_F l \simeq 1$). Such a localization phenomenon occurs when $R_\square$ approaches the critical value $R_\square^{\mathrm{Tr}} = 25.8$ kΩ [12]. When $R_\square^{\mathrm{Tr}} = h/4e^2$ these systems are termed bosonic since the carriers are treated as pairs, and when $R_\square^{\mathrm{Tr}} = h/e^2$ these systems are termed fermionic since the carriers are treated as single electrons.

The normal-state resistance behavior as a function of temperature appears to be quite different for the two classes of superconductors. For LTSs, the derivative $\Delta R/\Delta T$ is positive, though very small in most cases, over the whole temperature range, while, on the contrary, negative values have been measured at low temperatures for many HTSs [13]. The bosonic nature of the MIT for the LTSs is widely accepted. However, the critical normal-state sheet resistance frequently reported in the literature [14,15] for HTSs raised concerns about the nature of the MIT in such systems because it was usually larger than $h/4e^2$. A conclusive picture of the MIT in HTS systems is still missing, even though studies have been done on several different high-T_c cuprates, such as irradiated YBaCuO and BiSrCaCuO [16], Zn-doped LaBaCaCuO [17], Y-doped BiSrCaCuO [18], Ce-doped NdCuO [19], oxygen-deficient YBaCuO single crystals [20], Pr-doped or Zn-doped YBaCuO [21,22], and ultrathin DyBaCuO films [23].

An important uncertainty related to the structural features of all HTSs [24] is the ambiguity in the definition of the effective thickness t of the conducting layer. This value, which is necessary to calculate $R_\square$ from the resistivity ρ value, has been variably chosen as half of the c-axis lattice constant ($t = 15$ Å) in $Bi_2Sr_2Y_xCa_{1-x}Cu_2O_8$ [18], as the whole c-axis lattice constant ($t = 11.8$ Å) in $YBa_2Cu_3O_{7-x}$ [20], or as the spacing between CuO_2 layers ($t = 6$ Å) in $Nd_{2-x}Ce_xCuO_4$ [19]. This ambiguity is crucial for judging whether the bosonic or fermionic explanation of the 2D MIT is realized in practice. Ultrathin artificial cuprate structures, as discussed here, offer unique

opportunities to define the proper regime. In a previous work on the HTS superlattices $(BaCuO_{2+x})_m/(CaCuO_2)_n$ (Cbcco–$m \times n$) both the dependence of the critical temperature and the electrical transport properties on n for n ranging from 1 to 15 (with $m = 2$) have been investigated [25]. These artificial structures were grown by pulsed laser deposition in order to stack in sequence individual nonsuperconducting layers of $BaCuO_{2+x}$ and $CaCuO_2$. In the Cbcco–$m \times n$ unit cell, the superconducting block consists of n epitaxial layers of $CaCuO_2$ while the m epitaxial layers of $BaCuO_{2+x}$ play the role of a charge reservoir block [26]. In the case of samples with ultrathick superconducting blocks [25], the ambiguity in determining the critical normal-state sheet resistance at which the MIT occurs was minimal. To calculate $R_\square$ for each superlattice, the formula $R_\square = \rho/t$ was used, where t can be either the superlattice modulation length Λ or the thickness of the Ca-based infinite layer (IL) block alone. For the insulating Cbcco–2×14 superlattice, t is equal to 44.8 Å if we consider the IL block alone or 53.6 Å for the whole superlattice cell. This leads to an uncertainty of about 15% on the $R_\square$ value. For comparison, in the case of YBCO, the whole unit cell is 3 times larger than the superconducting Y-based block. The critical temperature T_c versus the sheet resistance $R_\square$ for Cbcco ultrathick superlattices [25] showed that the MIT takes place for a sheet resistance of about $\simeq 26$ kΩ [27]. However, even if the ultrathick cuprate superlattices have shown a good reliability in the precise determination of $R_\square$ values at the MIT, a direct measure of $R_\square$ has been never performed on a single-layer HTS film.

Recently it has been shown that high-T_c superconductivity can be achieved in ultrathin $CaCuO_2$ layers at the surface of $SrTiO_3/Ba_{0.9}Nd_{0.1}CuO_{2+x}/CaCuO_2$ and in the trilayered $Ba_{0.9}Nd_{0.1}CuO_{2+x}/CaCuO_2/Ba_{0.9}Nd_{0.1}CuO_{2+x}$ heteroepitaxial structures [28,29]. In order to obtain a more stable structure for such ultrathin structures, 10% of the Ba atoms are substituted by the trivalent Nd cations, slightly increasing the compensation of the electrical charge. Both the structures consist of only one superconducting Ca-based block of N layers of $CaCuO_2$. However, in the case of the bi-layered structures, the Ca-based block is grown on top of a single Ba-based block of M layers of $Ba_{0.9}Nd_{0.1}CuO_{2+x}$, while in the case of the trilayered structures, the Ca-based block is sandwiched between two Ba-based blocks. From now on, we will refer to these as the Cbcco–M/N and the Cbcco–$M/N/M$ structures, respectively. Here we show that such a superconducting ultrathin structure allows a direct measurement of $R_\square$ in a HTS system, clarifying some important issues regarding the MIT in HTS systems.

A preliminary argument to be addressed is the distribution of the electrical charge coming from the charge reservoir block within the superconducting block. In Cbcco–$2 \times n$ structures, the thickness of the superconducting blocks has been varied over a wide range, well beyond the possibility offered by conventional HTS materials. n varies from 1 to 15 while in standard HTS $n \leq 3$. Among the Cbcco–$2 \times n$ structures, the Cbcco–2×2 superlattices proved to be optimally doped and showed the highest superconducting transition temperature with zero resistance above 80 K. For thicker $CaCuO_2$ blocks the critical temperature decreases until for $n > 11$ the artificial structure is no longer superconducting. Such an effect was explained by considering the decrease of the effective carrier concentration per CuO_2 plane in thick Ca-based blocks. This result is consistent with a picture where holes injected from the charge reservoir block do not localize at the interfaces, but rather distribute quite homogeneously over the whole superconducting block. This can be confirmed by plotting T_c vs the number of CuO_2 planes [25] in terms of "*carriers per plane*". For a uniform charge distribution within the superconducting block, the carrier concentration per CuO_2 plane is simply inversely proportional to the number of CuO_2 planes (Fig. 1).

Additional support comes from the similarity between the plot of T_c vs the number of CuO_2 planes and the universal phase diagram for the high-T_c superconductors [30–32] (see the dotted line in Fig. 1). In the case of charge localization at the interfaces between the Ba-based and the Ca-based blocks, one would expect a saturation of the critical temperature value for a sufficiently thick IL block, as in the case of twin-planes superconductivity. We find instead the maximum value of $T_c = 80$ K in the case of $(BaCuO_{x+2})_2/(CaCuO_2)_2$ (2×2 superlattice), which has the optimal doping value $p = 0.18$–0.19 holes per CuO_2 plane [33]. In analogy with the Cbcco–$m \times n$ superlattices, we can drive the ultrathin Cbcco–M/N heteroepitaxial structures through the MIT by increasing the number of conducting $CaCuO_2$, thus decreasing the doping level for a single $CaCuO_2$ layer. R(T) measurements were performed by the standard four-probe pulse-reverse dc technique. Contacts were made by silver epoxy directly onto the substrate before the film deposition, in order to avoid any

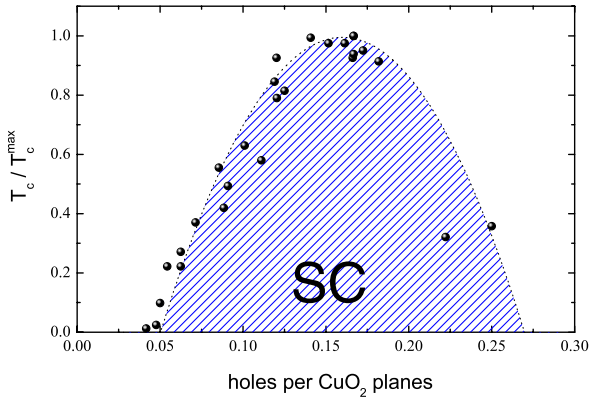

FIG. 1 (color online). Critical temperature T_c behavior (normalized to the maximum value $T_c^{max} = 80$ K) as a function of the carrier (holes) concentration per CuO_2 plane. The universal bell-shaped curve of superconducting (SC) phase vs doping is also plotted as a dotted line.

chemical reaction between the film and the solvent in the silver epoxy. All the ultrathin structures were measured using the Van der Pauw configuration [34]. The $R_\square$ was estimated as $(f \cdot \pi R_{\text{mean}}/\ln 2)$, where R_{mean} is the mean value of the Van der Pauw contacts' geometry (see the two configurations in the lower left panel of Fig. 2) and f is a prefactor value depending on R_a/R_b [34]. Because the R_a/R_b ratio has been found smaller than 3–4 for all samples, for sake of simplicity we set $f = 1$ for all the samples, resulting in a maximum overestimate of the absolute value of about 15%. In Fig. 2 the $R_\square$ behavior as a function of the temperature is displayed for Cbcco–$5/N$ with $N = 0.66$ and 1.0. In the case of $N = 0.66$, the number of laser shots on the $CaCuO_2$ target was $2/3$ of those required for $N = 1.0$. The accuracy of the thickness calibration was previously demonstrated by diffraction and reflectivity measurements with synchrotron radiation [35].

Comparison between the temperature dependence of $R_\square$ of the Cbcco–$5/0.66$ and Cbcco–$5/1$ structures suggests that the contribution to the normal-state resistance of the Ba-based block, which is more than 5 times thicker than the Ca-based block, can be neglected. The two structures only differ by a single $CaCuO_2$ layer. However, the resistance value measured in the Cbcco–$5/1.0$ structure is almost one-order of magnitude smaller than in the case of the Cbcco–$5/0.66$ structure, consisting in unconnected $CaCuO_2$ islands grown on the Ba-based block. This leads us to conclude that the change in the resistance value is primarily due to the single $CaCuO_2$ layer, which shows a higher conductivity compared to the Ba-based block.

This result is particularly interesting in view of a comparison between the $CaCuO_2$ alone and that grown on top of a Ba-based CR block. The $R_\square$ vs temperature behavior of the $CaCuO_2$ parent compound is also reported in the inset of Fig. 2. The electrically well-compensated $CaCuO_2$ block alone shows a strongly insulating behavior. In contrast, $CaCuO_2$ doped by a Ba-based block results in the highest electrical conductivity, possibly because of external doping in a well-ordered material.

Here we stress that the R(T) measurements of a single $CaCuO_2$ layer in the Cbcco–$5/1$ structure is a direct measurement of 2D-$R_\square$. The R(T) behavior was investigated in the Cbcco–$5/N$ structures with N varying from 1 to 6, thereby keeping the Ba-based block thickness constant while varying the superconducting block. Assuming a uniform distribution of the carrier concentration, the N $CaCuO_2$ layers can be considered as N equivalent CuO_2 conducting parallel planes. In analogy with the Cbcco–$2 \times n$ superlattices, the disappearance of the superconductivity for samples with thick enough $CaCuO_2$ blocks indicates that the carrier density decreases with increasing N. In contrast to all previous measurements, we can evaluate the single CuO_2 sheet resistance by simply multiplying the resistance of the Cbcco–$5/N$ structures by a factor N. The $R_\square$ versus temperature behavior along the Cbcco–$5/N$ series is shown in Fig. 3.

Again, as a consequence of the decrease of the carrier concentration per single layer, the $R_\square$ resistance increases with N. The $R_\square$ behavior near room temperature is shown in the inset of Fig. 3. The MIT occurs for a $R_\square$ value between the superconducting Cbcco–$5/4$ and the insulating Cbcco–$5/5$ structure values. More precisely, taking into account the 15% maximum overestimate on the absolute value of the $R_\square$ (previously discussed), the MIT occurs for a $R_\square$ value in the range between 25.2 ± 2.0 kΩ and 32.8 ± 2.7 kΩ for the Cbcco–$5/4$ and the Cbcco–$5/5$ structures, respectively. Such a value of $R_\square$ for MIT is in good agreement with the 2D quantum resistance value $h/e^2 = 25.8$ kΩ.

Further proof of the validity of such an approach is given by the analysis of the $R_\square$ for the Cbcco–$5/2/5$ trilayered structure, investigated both by transport measurements [29] and by scanning squid microscopy [36]. In that case, the effective thickness t is very different if one chooses to

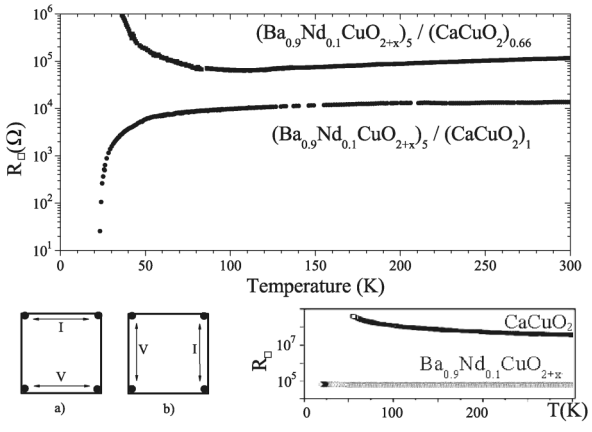

FIG. 2. (upper part) The sheet resistance $R_\square$ vs temperature for the $(Ba_{0.9}Nd_{0.1}CuO_{x+2})_5/(CaCuO_2)_N$ (with $N = 0.66, 1$). (lower part) On the right, the schematic diagram of the Van der Pauw geometrical configurations of the two pads for current injection is reported; on the left, the $Ba_{0.9}Nd_{0.1}CuO_{x+2}$ and $CaCuO_2$ parent compounds' behavior is also reported.

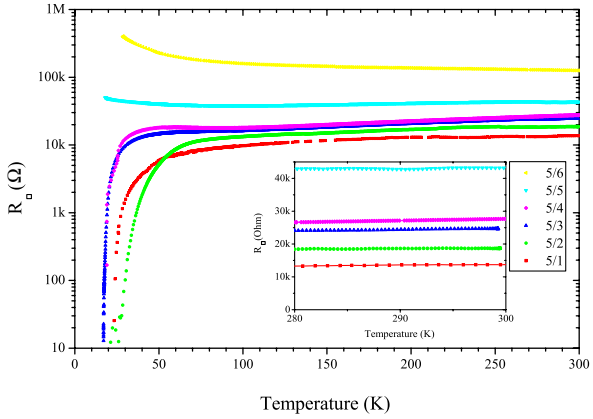

FIG. 3 (color online). $R_\square$ vs temperature behavior, along the $(Ba_{0.9}Nd_{0.1}CuO_{x+2})_5/(CaCuO_2)_N$ series (with N varying from 1 to 6). In the inset, the $R_\square$ behavior is magnified in proximity of the room temperature.

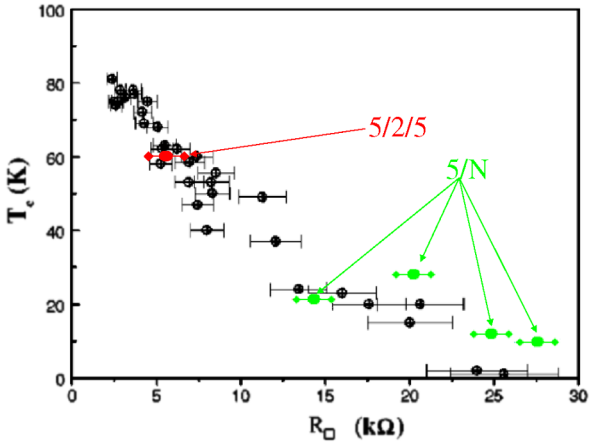

FIG. 4 (color online). Critical temperature T_c versus the sheet resistance $R_\square$ for ultrathick Cbcco–$2 \times n$ superlattices [25] (black dots), and for ultrathin Cbcco–$5/N$ [28] (green dots), and Cbcco–$5/2/5$ [29] (red dot) structures.

consider the IL-layer thickness alone (6.4 Å) or the whole structure thickness (48.9 Å). In agreement with the assumptions made for the Cbcco–$5/N$ structures as well as for the trilayered ultrathin structures, we consider just the $(CaCuO_2)_2$ layer as the truly superconducting block. Based on such an assumption, the $R_\square$ value for the Cbcco–$5/2/5$ sample that shows a critical temperature $T_c = 60$ K [29] is found to be about 5.4 kΩ. Such a value is in very good agreement with the general T_c vs $R_\square$ behavior found for the bilayered Cbcco–$5/N$ ultrathin structures and the Cbcco–$2 \times n$ ultrathick superlattices (all plotted in Fig. 4).

In conclusion, the metal-insulator transition has been investigated in terms of room temperature 2D $R_\square$ values. Because of the complex structural features of HTS materials, the $R_\square$ value strongly depends on the thickness chosen for the conducting layer, giving rise to an ambiguity in evaluating the sheet resistance. We have shown that it is indeed possible to directly measure the 2D $R_\square$ sheet resistance in the bilayered Cbcco–M/N and trilayered Cbcco–$M/N/M$ ultrathin (overall thickness smaller than 50 Å) heteroepitaxial structures. In agreement with a previous study [25], the metal-insulator transition occurs for a critical value of $R_\square$ close to the 2D quantum resistance value h/e^2, strongly supporting the fermionic explanation for the MIT in the HTS cuprate system. Moreover all data confirm the assumption that each CuO_2 layer forms a 2D superconducting sheet within the superconducting block, which can be described as weak-coupled equivalent CuO_2 sheets in parallel.

The authors are grateful to V. G. Kogan and J. R. Kirtley for fruitful scientific discussions. This work has been partially supported by MIUR under the project "Macroscopic Quantum Systems: Fundamental Aspects and Application of Non Conventional Josephson Structures".

[1] Y. Liu, D. B. Haviland, B. Nease, and A. M. Goldman, Phys. Rev. B **47**, 5931 (1993); Y. Liu *et al.*, Phys. Rev. Lett. **67**, 2068 (1991); D. B. Haviland, Y. Liu, and A. M. Goldman, Phys. Rev. Lett. **62**, 2180 (1989); H. M. Jaeger, D. B. Haviland, A. M. Goldman, and B. G. Orr, Phys. Rev. B **34**, 4920 (1986); A. M. Goldman and N. Markovic, Phys. Today **51**, No. 11, 39 (1998).
[2] L. J. Geerligs *et al.*, Phys. Rev. Lett. **63**, 326 (1989).
[3] A. J. Rimberg *et al.*, Phys. Rev. Lett. **78**, 2632 (1997).
[4] V. Ambegaokar, B. I. Halperin, and J. S. Langer, Phys. Rev. B **4**, 2612 (1971).
[5] D. Berman, B. G. Orr, H. M. Jaeger, and A. M. Goldman, Phys. Rev. B **33**, 4301 (1986).
[6] B. G. Orr, H. M. Jaeger, A. M. Goldman, and C. G. Kuper, Phys. Rev. Lett. **56**, 378 (1986).
[7] A. Schmid, Phys. Rev. Lett. **51**, 1506 (1983).
[8] M. P. A. Fisher, Phys. Rev. Lett. **57**, 885 (1986).
[9] B. G. Orr, J. R. Clem, H. M. Jaeger, and A. M. Goldman, Phys. Rev. B **34**, 3491 (1986).
[10] S. Chakravarty, G.-L. Ingold, S. Kivelson, and A. Luther, Phys. Rev. Lett. **56**, 2303 (1986).
[11] A. O. Caldeira and A. J. Leggett, Ann. Phys. (N.Y.) **149**, 374 (1983).
[12] S. K. Tolpygo *et al.*, Phys. Rev. B **53**, 12 454 (1996).
[13] M. R. Mohammadizadeh and M. Akhavan, Supercond. Sci. Technol. **16**, 1216 (2003).
[14] K. Semba and A. Matsuda, Phys. Rev. Lett. **86**, 496 (2001).
[15] S. Oh, T. A. Crane, D. J. Van Harlingen, and J. N. Eckstein, Phys. Rev. Lett. **96**, 107003 (2006).
[16] F. Rullier-Albenque *et al.*, Physica (Amsterdam) **C254**, 88 (1995).
[17] R. Singh *et al.*, Phys. Rev. B **55**, 1216 (1997).
[18] D. Mandrus, L. Forro, C. Kendziora, and L. Mihaly, Phys. Rev. B **44**, 2418 (1991).
[19] S. Tanda, M. Honma, and T. Nakayama, Phys. Rev. B **43**, 8725 (1991).
[20] G. T. Seidler, T. F. Rosenbaum, and B. W. Veal, Phys. Rev. B **45**, 10 162 (1992).
[21] G. A. Levin *et al.*, Phys. Rev. Lett. **80**, 841 (1998).
[22] T. R. Chien, Z. Z. Wang, and N. P. Ong, Phys. Rev. Lett. **67**, 2088 (1991).
[23] T. Wang *et al.*, Phys. Rev. B **43**, 8623 (1991).
[24] H. Shaked *et al.*, *Crystal Structures of the High T_c Superconducting Copper-Oxides* (Elsevier, Amsterdam, 1994).
[25] G. Balestrino *et al.*, Phys. Rev. B **62**, 9835 (2000).
[26] G. Balestrino and A. Tebano, Supercond. Sci. Technol. **16**, R29 (2003).
[27] B. L. Altshuler, D. L. Maslov, and V. M. Pudalov, Physica (Amsterdam) **E9**, 209 (2001); Phys. Status Solidi B **218**, 193 (2000).
[28] G. Balestrino *et al.*, Phys. Rev. B **66**, 094505 (2002).
[29] G. Balestrino *et al.*, Appl. Phys. Lett. **79**, 99 (2001).
[30] M. Thinkam, *Introduction to Superconductivity* (McGraw-Hill, New York, 1996), 2nd ed..
[31] H. Takagi *et al.*, Phys. Rev. Lett. **69**, 2975 (1992).
[32] S. Chakravarty, H.-Y. Kee, and K. Völker, Nature (London) **428**, 53 (2004).
[33] M. Putti *et al.*, Phys. Rev. B **69**, 134511 (2004).
[34] L. J. van der Pauw, Philips Res. Rep. **13**, 1 (1958).
[35] C. Aruta *et al.*, J. Appl. Phys. **94**, 6991 (2003).
[36] F. Tafuri *et al.*, Phys. Rev. Lett. **92**, 157006 (2004).